



## **PATH PLANNING FOR AUTONOMOUS UNDERWATER VEHICLES IN REALISTIC OCEANIC CURRENT FIELDS: APPLICATION TO GLIDERS IN THE WESTERN MEDITERRANEAN SEA**

B. Garau<sup>1\*</sup>, M. Bonet<sup>1</sup>, A. Alvarez<sup>2</sup>, S. Ruiz<sup>1</sup> and A. Pascual<sup>1</sup>

Received 22 September 2008; received in revised form 29 September 2008; accepted 15 April 2009

### **ABSTRACT**

Autonomous Underwater Vehicles (AUVs) usually operate in ocean environments characterized by complex spatial variability which can jeopardize their missions. To avoid this, planning safety routes with minimum energy cost is of primary importance. This work revisits the benefits, in terms of travelling time, of path planning in marine environments showing spatial variability. By means of a path planner presented in a previous paper, this work focuses on the application to a real environment of such techniques. Extensive computations have been carried out to calculate optimal paths on realistic ocean environments, based on autonomous underwater glider properties as the mobile platform.

Unlike previous works, the more realistic and applied case of an autonomous underwater glider surveying the Western Mediterranean Sea is considered. Results indicate that substantial energy savings of planned paths compared to straight line trajectories are obtained when the current intensity and the vehicle speed are comparable. Conversely, the straight line path between starting and ending points can be considered an optimum path when the current speed does not exceed half of the vehicle velocity. In both situations, benefits of path planning seem dependent also on the spatial structure of the current field.

**Keywords:** path planning, autonomous underwater vehicles, ocean variability.

---

<sup>1</sup> Instituto Mediterraneo de Estudios Avanzados, Mallorca, Spain. <sup>2</sup> NATO Undersea Research Centre, La Spezia, Italy. \*Corresponding author (tomeu.garau@uib.es) IMEDEA (UIB-CSIC). C/Miquel Marques, 2107190, Esporles, Islas Baleares, Spain.

## INTRODUCTION

Autonomous underwater vehicles (AUVs) must frequently operate in ocean environments characterized by complex spatial variability (Schmidt and Bovio, 2000). This spatial complexity is induced by the turbulent nature of the ocean, described by the continuous change of a wide range of spatial and time scales. Energetic flows induced by tides and topographic perturbations, instabilities and currents induced by local wind effects, are only few examples of ocean variability. This variability can strongly perturb the development of AUVs operations (Galea, 1999). In particular, AUVs usually encounter strong current fields in the marine environment that can jeopardize their missions. Determining and predicting ocean currents is then a fundamental requirement to optimize certain aspects of the AUV's performance, specifically when vehicles have to operate energy-exhaustive missions in ocean areas characterized by comparatively strong currents. In such cases, it is of primary importance to plan safety routes with minimum energy cost.

Nowadays, several systems can provide an estimation of the existing current field in a certain region. Numerical ocean models can provide nowcasts and forecasts of ocean variability (Holland and McWilliams, 1987). A typical numerical ocean model consists of finite difference equations representing the momentum, heat and salt balance in a determined area. These equations are integrated forward in time to predict the time evolution of the horizontal and vertical structure of the fluid flow as well as the temperature and salinity within the domain, given the wind stresses and buoyancy forcing at the sea surface. Satellites can also provide current fields derived from their observations of the sea level. The procedure consists of merging into one map the sea level anomalies measured by altimetric satellites along their tracks. Current fields can be derived applying the geostrophic assumption on the resulting merged map. Information of the environmental current field, obtained either from the ocean models or from satellites observations, can be incorporated into existing path finding algorithms to plan safety routes with minimum energy cost (Alvarez and Caiti, 2001).

Traditionally in AUVs, path planning has been related to safety conditions. The path should be devoid of known obstacles or hazardous areas. Different computational methods were employed to plan safety paths for AUVs. Warren (Warren, 1990) used potential field algorithms to solve the path planning problem. The algorithm used artificial potential fields applied to the obstacles and goal positions, employing the resulting field to influence the path of the AUV. Graph searching techniques were employed by Carroll et al. (Carroll et al, 1992) for AUV path planning. In this case, a chart or graph is produced showing free space where no collision will occur and forbidden spaces where a collision will occur. Based on this graph, a path is selected by piecing together the free spaces or by tracing around the forbidden spaces. Techniques such as case-based reasoning (Vasudevan and Ganesan, 1996) and genetic algorithms (Sugihara and Yuh, 1997) have also been applied to the motion planning for underwater robotic vehicles.



Alvarez and Caiti (Alvarez and Caiti, 2002) employed dynamic programming to carry out a systematic simulation study of the energy savings obtained through optimal AUV path planning, taking into account the spatial structure of the current velocity field. The study had the objective of putting in relation the spatial scales of the current field variability with the expected energy saving due to the optimized path planning. Results indicated a substantial energy saving, as compared to straight line paths, when ocean eddy structures were greater than one-third of the total crossing distance. Finally, the problem of AUV mission planning optimizing the energy cost in ocean environments with real current fields was considered by Alvarez et al. (Alvarez, Caiti and Onken, 2004). The developed planning algorithm integrated the current predictions obtained from the Harvard Ocean Prediction System (HOPS) (Robinson et al, 1996) to an evolutionary navigator, providing the path with minimum energy requirements. In these studies incorporating the current field, the AUV speed with respect to the bottom was assumed to be constant. Thus, the considered AUV was able to adapt its speed depending on the current field where it was immersed, being the total speed constant through the planned path.

Recently, Garau et al (Garau, Alvarez and Oliver, 2005) considered a more common situation on actual AUVs, where the thrust power is usually kept constant during the mission. Thus, in the usual situation the optimization of energy consumption agrees with finding the minimum-time path. This defines an optimization problem in oceans with spatial variability, different from the previously studied. Minimum-time paths were computed in simulated ocean basins with different eddy sizes and current speeds. Results showed the path planner performance depends on different parameters like current strength or eddy size.

In this article we apply the proposed techniques in the abovementioned paper, in the more realistic and applied case of current fields derived from different models as well as satellite altimetry. The real path followed by an actual platform is also compared to the planned path.

The paper is organized as follows: Section II details the designing of the route planner while Section III describes the different ocean environments employed in the simulations. A real platform is presented in section IV. Results from two different deployments are shown in Section V and discussed in Section VI.

## THE PATH PLANNER

The presented path planner considers the case of AUV motion on the horizontal plane. This simplification is justified by the interest in the effect of horizontal ocean structures on AUVs because vertical motions in ocean structures are generally negligible. Moreover, the scales of variability that can be forecasted by models or observed from satellites are large enough to suppose that the main movement of the vehicle will be on a horizontal plane.



The dimensions of the AUV are considered much smaller than the dimensions of the ocean basin and ocean structures. Thus static route planning, which does not account for the AUVs dynamics, is appropriate. Consider the two-dimensional underwater environment discretized in space over a grid. Any point in the grid defines a node whose coordinates units will be measured in degrees (latitude and longitude), a coherent decision taking into account the size of the region to be considered. This grid, conversely to the previous version of the path planner, can be regular or irregular, and it can even be a triangular mesh like the ones produced by finite element methods. A path between a starting node and a destination node is defined through a sequence of nodes which are interconnected, and it is made by straight-line segments connecting any two adjacent nodes. In practice, it is assumed that the AUV navigation is defined through via-points that are the nodes of the grid. A current velocity vector is defined at any point in space.

Within this setting, the path planning problem can be enunciated as follows: given a start node  $s$ , a destination node  $d$  and a current velocity field, find a path such that the time required for a vehicle travelling along the path at a constant thrust power is minimum, subject to the constraints that the path does not intersect any solid obstacle.

The travelling time required by a given path is evaluated computing and adding up the time required covering each segment constituting the path. Consider a segment connecting two nodes  $n_{i-1}n_i$  of any arbitrary path; let  $d_i$  indicate its length, and let  $\vec{e}_i$  be a unitary vector oriented along the segment in the direction of desired motion of the vehicle. At any point  $(x,y)$  along the segment the vehicle must have a nominal velocity  $\vec{v}_i(x,y)$  given by:

$$\vec{v}_i(x,y) = \vec{v}_r(x,y) + \vec{v}_c(x,y), \forall (x,y) \in n_{i-1}n_i \tag{1}$$

where  $\vec{v}_r$  is the speed of the vehicle relative to the current,  $|\vec{v}_r|$  is constant and proportional to the cubic root of the constant thrust. The time to cross the segment is given by,

$$t_i = \frac{|d_i \vec{e}_i|}{|\vec{v}_i|} \tag{2}$$

and the total travelling time of the path is finally given by the summation  $\sum_1^m t_i$ .

Computational difficulties on evaluating expression (2) appear when current speeds are different in the surrounding nodes. In these cases, a unique velocity cannot be defined for the entire segment. A recursive approach has been implemented



to overcome the problem. The segment is split into sub-segments until the difference between the interpolated current speeds at the end points of each subsegment, do not exceed a given threshold. Then, equation (2) is applied to each sub-segment with a current speed obtained from averaging the current velocities at the subsegment end points. The total time required to cover the segment is the summation of the travelling times of each sub-segments.

An A\* algorithm has been implemented as a search engine to find the optimum path in a given ocean environment. The traditional Euclidean distance between the field point and the destination goal, divided by the maximum possible nominal speed (maximum current speed plus the vehicle speed) was employed like heuristic function. This election ensures that the heuristic cost will be always lower than the actual cost to reach the goal from a given node and thus, the optimum solution is guaranteed. Moreover, previous works have showed that this simple heuristic function guides the search, reducing the computation time.

An improvement applied on the initial path planner is made on the conversion from the initial grid to graph, which is the input to the path planner. While the previous version considered the typical 8-connectivity to generate the edges between nodes of the grid, in this study it has been increased to 16-connectivity. This is a subset of the 24-connectivity, dismissing the edges that represent a path reproducible exactly with edges from the 8-connectivity. This improvement provides more flexibility to the path planner to adapt the path to the current direction. It also increases the number of edges in the searching graph, increasing the computational effort. Nevertheless, the heuristic function guides the search and helps in not increasing the computation time due to the larger number of edges.

In order to test the path planner performance in the work presented by Garau et al (Garau, Alvarez and Oliver, 2005), the current fields used for their simulations were obtained from a streamfunction field  $\Psi(x,y)$  randomly generated from a specific isotropic power spectrum peaked at determined scales with random phases. This procedure allows the generation of current fields with controlled features. Therefore, it is feasible to study the path planner performance based on the predominating scales over the field, their maximum current intensity or any other parameter of interest. The current fields were defined on a regular grid with a fixed distance between grid points, expressed in meters, for easiness of computation.

## REALISTIC OCEAN ENVIRONMENTS

While the abovementioned work evaluated path planner performance, this work presents the application of the same path planner on realistic situations. The previous assumptions of a regular grid points equidistant and the randomly generated stream function fields are not used. Instead of a regular grid, a graph is used, allowing either for regular or irregular grids, as well as meshes produced by finite elements



methods. These changes are introduced to improve the adaptability of the path planner to different sources of oceanographic information.

Oceanographic environmental information can be extracted either from in-situ or remote observations, or numerical forecast models. The oceanographic observations are characterized by their spatial distribution as point time-series, trajectories, profiles or 2D grids. Examples of that are moorings, gliders, CTD ship cruises or satellite observations, respectively. The numerical models usually provide 2D or 3D information about marine environment properties. For the case of the path planner, the gridded data is the required information, and so, several trials will be done with satellite observations as well as forecast model outputs.

Several model outputs and satellite observations can be used for the realistic path planning. Examples of these sources are, among others, MFS (Mediterranean Forecast System), IFOSY (IMEDEA Forecast System), ESEOO (Establecimiento Español de un Sistema de Oceanografía Operacional) or AVISO.

MFS is the output of the numerical forecast model that has been setup and is running operationally at INGV (Istituto Nazionale di Geofisica e Vulcanologia). It uses GFDL-MOM (Geophysical Fluid Dynamics Laboratory-Modular Ocean Model, Pakanowsky et al., 1990) which is a three-dimensional primitive equation ocean general circulation model designed by Bryan, (1969) and Cox (1984). MFS provides forecasts outputs on a regular grid with a resolution of  $1/16^\circ$  that covers the whole Mediterranean Sea.

AVISO provides near real time images of absolute dynamic topography and geostrophic currents obtained from a process of optimal interpolation combining all the available altimeters (Jason-1, Envisat, Geosat Follow-On). The absolute dynamic topography is obtained through the sum of the sea level anomaly measured by the altimeter plus a mean dynamic topography (Rio et al., 2007). Currents are computed applying the geostrophic approximation. The spatial resolution of this product is  $1/8^\circ$ .

Besides the different spatial resolution and limits, the heterogeneity of data sources is an issue to be tackled. The Centro Operacional de Datos Oceanográficos (CODO) located in Mallorca as part of the Tecnologías Marinas, Oceanografía Operacional y Sostenibilidad (TMOOS) department of the Institut Mediterrani d'Estudis Avançats (IMEDEA) is working on the standardization of the data from different sources in the Western Mediterranean Area for its distribution. The path planner has been tested with information resulting of this work. This standardization allows using different data sources over the same area without changing the path planner software.

An international data format standard for the oceanographic data has been adopted. NetCDF (network Common Data Format) is a set of software libraries and machine-independent data formats that support the creation, access, and sharing of array-oriented scientific data. The oceanographic data is associated to a geospatial location that can be stored in the NetCDF files. However, the format does not



determine the relationship between the data and its spatial distribution in terms of latitude and longitude or depth. The conventions for climate and forecast (CF) metadata are designed to promote the processing and sharing of files created with the NetCDF API.

CF are increasingly gaining acceptance and have been adopted by a number of European projects and groups as a primary standard. The conventions define metadata that provide a definitive description of what the data in each variable represents, and the spatial and temporal properties of the data. This enables data users from different sources to decide which quantities are comparable, and facilitates building applications with powerful extraction, regridding, and display capabilities. Using data with these conventions makes it easier to the path planner for reading the input current fields. The path planner uses the NetCDF/CF format due to its advantage and because CF conventions generalize and extend other conventions on NetCDF such the COARDS conventions, thus, being backward compatible.

Besides the data format, the access mechanism to it has to be taken into account, since it tends to be distributed over internet and the datasets are relatively large. For the distribution of oceanographic data the most extended protocol is the OpenDAP (Open-source Project for a Network Data Access Protocol). OpenDAP is a framework that simplifies all aspects of scientific data networking. OpenDAP provides software which makes local data accessible to remote locations regardless of local storage format. The OpenDAP protocol allows the access to a concrete variable of the file without downloading the whole file. In the case of the path planner, the current fields are extracted from a remote file, and the software works with them as if the data was stored locally.

IMEDEA has a data catalog using THREDDS (TDS, Thematic Real-time Environmental Distributed Data Services) [<http://dataserver.imedea.uib-csic.es:8080/thredds>]. TDS is a web server that provides metadata and data access for scientific datasets, using OPeNDAP, OGC WMS and WCS, HTTP, and other data access protocols.

IMEDEA has been using a special type of AUV as an in-situ observing platform for several purposes. The platform is integrated in the CODO data management system as well as other platforms such as moorings, uses NetCDF/CF as data format delivery and its information is organized on the same Thredds catalogue as the models and the satellite information. This AUV, which is presented in the next section, and some of its missions have been used in this work to test the path planner performance.

## OCEANOGRAPHIC AUV PLATFORM

An underwater glider is a type of autonomous underwater vehicle (AUV) that uses small changes in its buoyancy in conjunction with wings to convert vertical



motion to horizontal, and thereby propel itself forward with very low power consumption. Gliders follow an up-and-down, sawtooth-like profile through the water, providing data on temporal and spatial scales unavailable to previous AUVs.

In the presented experiment the deployed platform was a Slocum shallow electric glider manufactured by Webb Research Corporation. The Slocum glider, named after Joshua Slocum, the first person to solo circumnavigate the world, is a torpedo shaped, winged vehicle that is 1.5 meters long, weighs 52 kilograms and has a hull diameter of 21.3 cm (Creed et al, 2002). The wings, made of composite material are mounted just aft of the centre of buoyancy.

There are three main hull sections plus wet fore and aft sections. The front wet section or nose dome houses a 200 kHz transducer for altimeter use. This section also has a hole on the centerline for large bore movement of water as is created by the displacement piston pump. The first main hull section contains the displacement piston pump, pitch vernier mechanism, altimeter electronics, ballast weights and a large alkaline battery pack that supplies power and serves as the mass moved by the pitch control during ascent and descent. The middle hull section encloses the science payload, additional energy and ballast weights. The third main hull section houses the back chassis that holds the navigation and communication electronics, the catalyst, the air pump system for the air bladder, battery power, vehicle controller, hardware interface board and attitude sensor.

A pressure transducer is ported through the aft end cap. The aft battery pack can be manually rotated for static roll offsets. The air bladder, steering assembly, burn wire, jettison weight and power umbilical are housed in the wet tail section. This section also has provisions for external trim weights and wet sensors. Protruding through the aft end cap and through the tail cone is the antenna fin support. This boom is a pressure proof conduit for the antenna leads and low noise amplifier for the GPS. Below the boom is a protected conduit for the steering motor linkage. Attached to the boom is the antenna fin.

Prior to a mission, the glider is ballasted to make it neutrally buoyant in the waters it has to operate in. To dive, the displacement piston pump moves water into the nose making the vehicle's nose heavy. To ascend, water is pushed out of the nose by the piston pump making the glider buoyant. The volume of water is approximately 233 cm<sup>3</sup>, and causes two effects on the glider: changes its buoyancy and moves the centre of gravity along the longitudinal axis of the vehicle. The buoyancy change induces on the glider a force that accelerates the vehicle in the vertical axis. This acceleration increases the glider vertical speed. The drag force, proportional to the square of the speed, also increases until an equilibrium point is reached. When both forces are equal, the glider vertical speed is kept constant through the dive or climb. It is designed to operate between the surface and 200 m of depth. During the ascent or descent, the glider moves the pitch batteries to fine adjust the centre of gravity and therefore the diving angle.



Typical values for its vertical speed are around 0.2 m/s. The vehicle is designed also to acquire a pitch angle close to  $26^\circ$ . Therefore, adding a small angle of attack (approx.  $1^\circ$ ) of the glider, the horizontal speed it can reach is  $\frac{0,2}{\tan(27)} \approx 0.4 \text{ m/s}$ .

This nominal speed, without taking currents into account, will be the one used by the path planner as the thrust produced by the vehicle.

The air bladder in the aft section provides buoyancy and stability while the glider is surfaced. The inflated air bladder also lifts the tail fin out of the water to facilitate communication of the glider with its Command Center. To steer the glider the back portion of the tail fin is moved as a controlled plane that acts as a rudder. Communication with the glider is done using line of sight radio frequency (RF) modem (FreeWave) for local high speed communications, ARGOS for a recovery beacon and Iridium for bi-directional satellite communications.

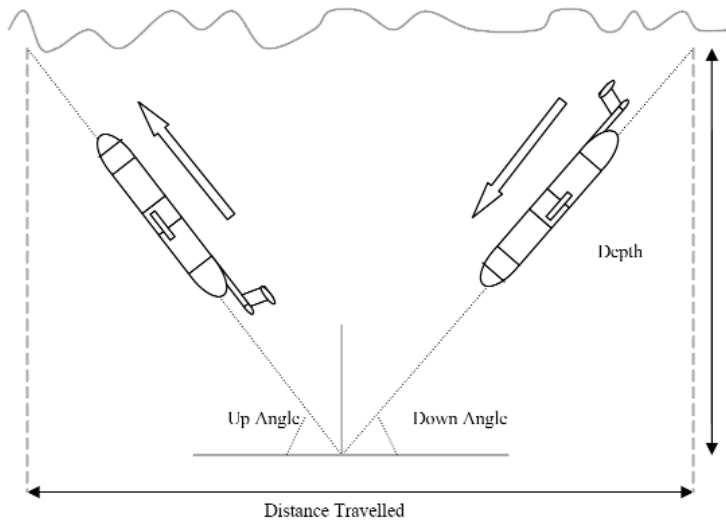


Figure 1. Schema of a glider inflection.

Deployment region and duration, dependent upon what scientific measurements are being taken and what type of communication is being used averages 30 days with a range of 1500 km. The deployment is defined as a set of waypoints that the glider has to navigate.

Glider navigation is done using GPS, internal dead reckoning and the altimeter. While underwater, the glider dead reckons its position relative to the water. When surfaced, the glider receives a precise location from its gps. Assuming that the dead reckoning and GPS are perfect, any errors between the gps fix and the final dead

reckoned position must be due to the currents fields. The glider can use the measured water current in its next underwater segment to navigate better.

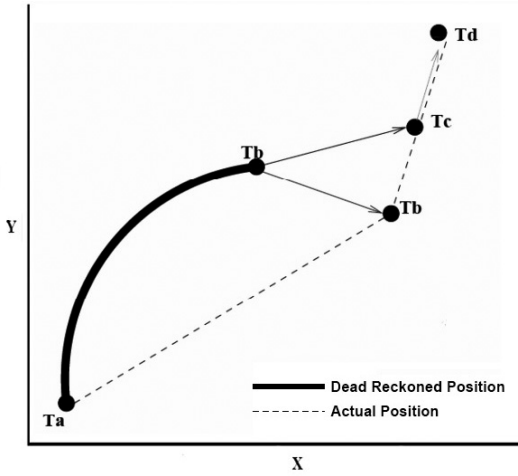


Figure 2. Schema of glider current estimation.

As shown in figure 2, at time  $T_a$ , the glider dives and surfaces at time  $T_b$ . The dotted line connecting  $T_a$  and  $T_b$  represents the actual path the glider performed underwater. The solid line linking  $T_a$  and  $T_b$  represent the dead reckoned trajectory of the glider.  $T_c$  represents the first GPS fix position. During this time, the glider drifts on surface due to the wind effect. To estimate this drift, the glider waits until  $T_d$  to fix a new GPS position. Assuming a constant surface drift, the glider is able to estimate the position where it surfaced. Then, it can compute the distance

between the dead reckoned position and the actual one in order to estimate the integrated drift while underwater.

## RESULTS

Previous works established that path planning provides substantial improvements when currents strengths are close to the AUV nominal speed. In this work, two different glider deployments have been considered to exemplify in a real scenario such conditions. First, a glider mission in the North of the Balearic Islands is shown to provide the case of weak currents. Also, a more interesting case in the Alboran Sea is shown, where the current intensities are even higher than the vehicle nominal speed.

### Missions and Scientific Goals

During the JASMIN cruise, performed in August 2008, between the 12<sup>th</sup> and the 27<sup>th</sup>, a coastal glider followed the JASOn satellite 70 track from MINorca to the Iberian Peninsula coast. This track is of particular interest because it runs perpendicular to the main oceanographic features in the Balearic Sea (Ruiz et al, 2008; Bouffard et al, 2009). The JASMIN cruise was conducted during the calibration phase of the satellite Jason-2 in the frame of the OST Proposal "Improvement, validation and merging of altimeter products for coastal and regional applications".

One month before, in the framework of the EU funded SESAME project, the same glider was deployed in July 2008, starting on the 2<sup>nd</sup> and ending on the 21<sup>st</sup>.



There were several specific objectives of this mission. One of them was to test the feasibility of the gliders technology usage in an area with intense current and high mesoscale variability. There was interest in exploring the feasibility of new assimilation techniques of data from different platforms (gliders, satellites, buoys, etc...) on high resolution models (2km) and also providing boundary conditions for SESAME numerical models. And finally, one of the major interests was to characterize the ocean variability and interaction between the Atlantic and Mediterranean water in the eastern Alboran Sea.

Figure 3 shows a general map of the region. Figure 4 presents two maps, one for each mission, showing the glider trajectories along with its own currents estimation during navigation. Endpoints are marked also in figure 4 as WP1 and WP2. The first segment of each mission covers the navigation between WP1 and WP2, while the second segment goes from WP2 to WP1

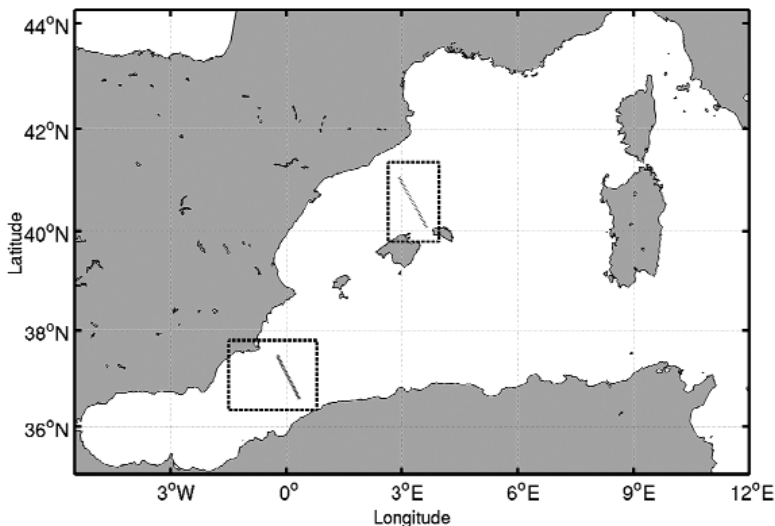


Figure 3. Map of WMED with the study areas marked with dashed lines and tracks marked with dotted lines.

### Environmental Conditions

During the two abovementioned missions, the Thredds catalogue provided access to environmental information. Several model outputs as well as altimetry maps were available to evaluate the current field the glider was to be operating in. Figures 5 and 6 show the current fields that were considered most relevant: MFS model output and altimetry maps. The maximum agreement between the current fields and the currents estimated by the glider is achieved with altimetry.

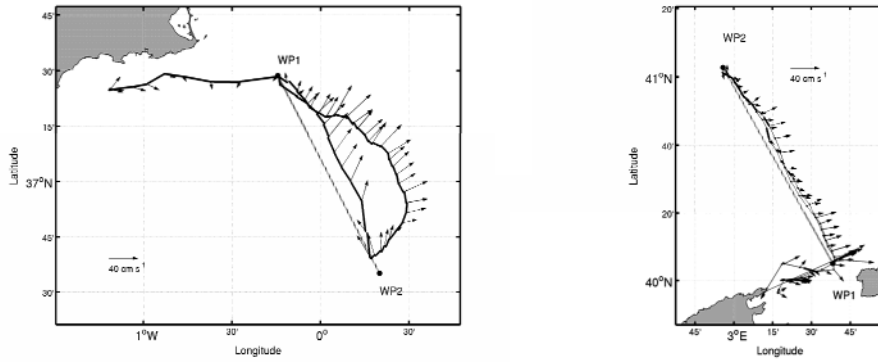


Figure 4. Glider trajectories and its estimated currents.

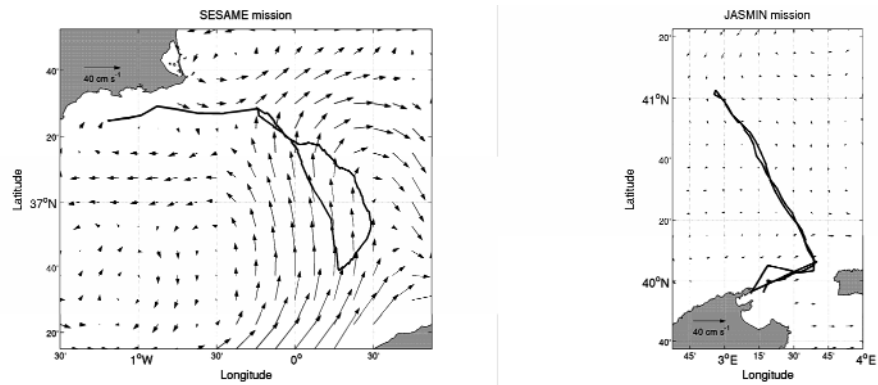


Figure 5. SESAME and JASMIN missions and altimetry derived current field.

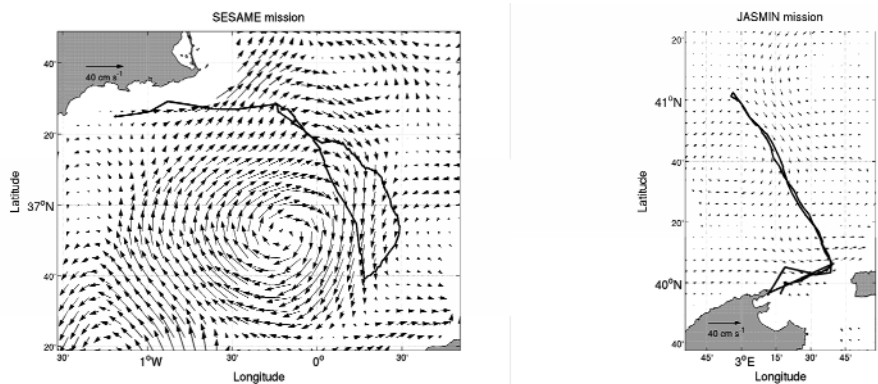


Figure 6. SESAME and JASMIN missions and MFS current field.



Figures 5 and 6 also show the trajectory that the glider followed when commanded to navigate along the satellite tracks. In the case of JASMIN mission, at the right hand side of both figures, currents were weak, and the glider was able to follow the expected straight line path when moving towards the northwest and southeast. However, during the SESAME mission, on the left hand side of both figures, a instability with strong currents was found on the glider path. This feature made the glider unable to follow the commanded route, and it was advected by the flow when performing the first segment. The second segment, where the glider moved north-west, was accomplished correctly by the glider since it was helped by the currents.

For JASMIN mission, the glider needed 5.53 days to travel the first segment (from south to north) and 4.45 days to make the second segment on its way back. During SESAME mission, the glider spent 7.73 days performing the first segment of the mission, and just 3.09 days for the second part. Moreover, the glider was unable to reach the southeast point, so the first segment was never completed as in the original mission design. The travelling time difference for the same segment performed in different directions provides an indication of the currents effects on the glider.

### Planned Paths

Using the current fields derived from altimetry and the MFS model output, minimum travelling time routes have been computed. Figures 7 and 8 show the results of the path planner.

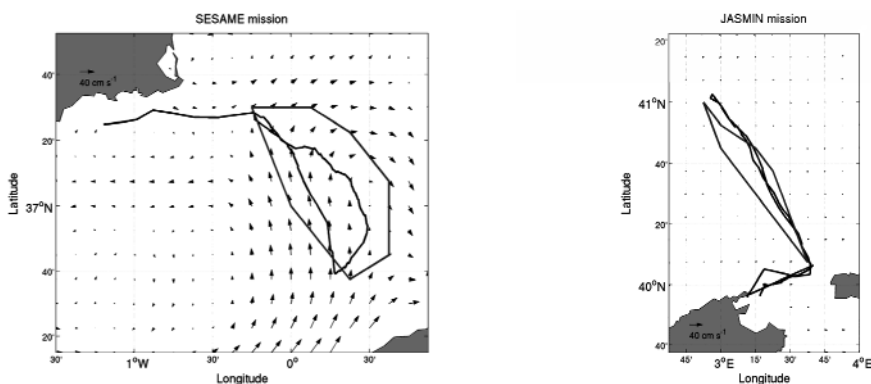


Figure 7. SESAME and JASMIN planned paths on altimetry derived current field.

Using ADT for JASMIN mission, the path planner provided a near-straight path. Thus, the improvement with respect to the straight line was almost zero. However, the estimated time to perform each segment was around 3.6 days. This fact is due to the difference between the ADT derived currents and the real currents felt by

the glider. Altimetry was providing currents in the correct direction but magnitude was lower.

When MFS model output was used for JASMIN mission, the path planner provided a slightly different pattern, but also close to the straight line. In this case, the path planner showed a higher improvement (close to 10%) than with ADT. The time estimation in this case was around 4.5 and 3.3 days for each segment, respectively. The explanation of the difference between results from each source is the fact that MFS was providing currents with higher intensity, but the circulation pattern was different. Therefore, the current intensities and their spatial distribution played an important role in both the shape of the path and the time estimation provided by the path planner.

Using ADT for SESAME mission, the path planner provided a very different path for both segments. While the first segment should be performed describing a curve, the second segment was to be performed in almost straight line path. The improvement with respect to the straight line was very high in the first segment (around 57%). For the second segment, as it was already straight, no improvement was made by the path planner.

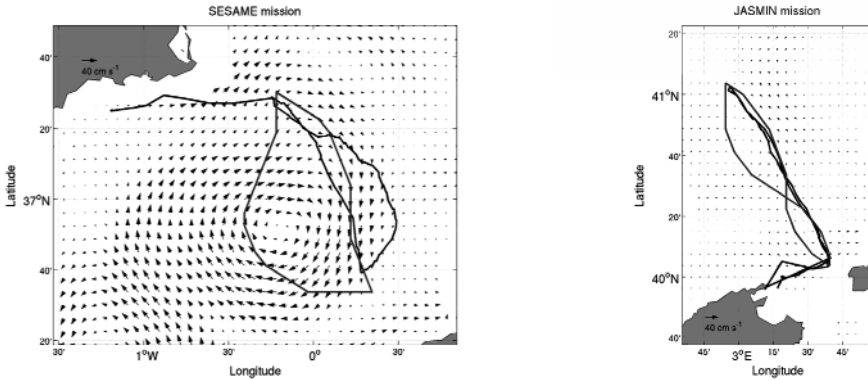


Figure 8. SESAME and JASMIN planned paths on MFS current field.

When MFS model output was used for SESAME mission, the path planner provided a very different pattern. In this case, results were dismissed because of the big misfit between glider estimated currents and current field. The model output was reproducing the eddy on the west of its position. Thus, the path planner results were computed over a wrong current field.

Given these two examples of deployments, it is reasonable to say that the path planner could not improve the glider performance in JASMIN mission, but could have improved travelling time significantly during SESAME mission, where the



currents were much stronger. This fact agrees with previous works conclusions about the path planner applicability.

## DISCUSSION

In this work, extensive computations have been carried out to calculate by means of the A\* based path planner, optimal paths (in terms of energy cost) in realistic ocean environments. Different sources of information have been used to capture the uncertainty of the current field used as input. The study is focussed on practical cases where the AUV develops a constant thrust independently of the current field where it is immersed. This substantially differs with previous works where the AUV was considered to adapt its speed to keep constant the total velocity with respect to the ground [9]. Now, minimum energy paths are also paths with minimum travel time being the problem more restrictive.

Concerning the benefits of path planning, results indicate that these are scarce when the vehicle velocity is clearly superior to the background current field. Substantial benefits of path planning are only obtained when the vehicle and current speeds are comparable. The velocity of present AUVs developing missions in the ocean is usually superior to current speeds normally found at the ocean. Nevertheless, path planning is required in those ocean areas characterized by strong currents. There, current intensities can reach values equal or even superior to the AUV velocity. In these cases, coupling a numerical ocean model or any other current field observation with a path planning algorithm constitutes an optimum solution to ensure the success and safety of the AUV mission.

The proposed techniques provide robustness and efficiency to AUVs. Robustness can be seen in the feasibility analysis of the path planner results. The reachability of a location is proven if the path planner is able to find a route to that destination. Thanks to the completeness of the searching algorithm, an impossible mission could be dismissed before deploying an AUV in a hazardous area. Efficiency plays an important role even when the straight path is feasible. Using the path planner, the scientists can replan the AUV trajectory to visit the same locations in a shorter time. This time saving allows for longer (in distance) or energy exhaustive (more sensors) missions.

## REFERENCES

- Alvarez, A. and Caiti, A. (2001): A genetic algorithm for autonomous underwater vehicle route planning in ocean environments with complex space-time variability. *Proceedings of the IFAC Control Applications of Marine Systems (CAMS 2001)*.
- Alvarez, A. and Caiti, A. (2002): Interactions of autonomous underwater vehicles with variable scale ocean structures. *Proceedings of the IFAC World Conference Systems*.
- Alvarez, A.; Caiti, A. and Onken, R. (2004): Evolutionary path planning for autonomous underwater vehicles in a variable ocean, *IEEE Journal of Oceanic Engineering* 29, no. 2, 12. pp. 418-429.
- Bouffard, J.; Roblou, L.; Birol, F.; Pascual, A.; Fenoglio-Marc, L.; Cancet, M.; Morrow, R. and Ménard, Y. (2009): Assessment of improved coastal altimetry strategies over the NMW Sea. Coastal altimetry. S. Vignudelli, A. Kostianoy, P. Cipollini and J. Benveniste Eds. Springer-Verlag. Submitted
- Bryan, K. (1969): A numerical method for the study of the circulation of the world ocean. *Journal of Computational Physics*, 4, 347-376.
- Carroll, K. P.; McClaran, S. R.; Nelson, E. L.; Barnett, D. M.; Friesen, D. K. and Williams, G. N. (1992): AUV path planning: An A\* approach. *Proceedings of the Symposium on AUV Technology (AUV92)*, pp. 3-8.
- Cox, M.D. (1984). A primitive equation, 3-dimensional model of the ocean. *GFDL Ocean Group Tech. Rep. N<sup>o</sup>. 1*, 143 pp.
- Creed, E.L.; Mudgal, C.; Glenn, S.M.; Schofield, O.M.; Jones, C.P. and Webb, D.C. (2002): Using a fleet of slocum battery gliders in a regional scale coastal ocean observatory, *Oceans '02 MTS/IEEE*, Volume 1, 29-31 Oct. 2002 Page(s):320 – 324
- Galea, A. M. (1999): Various methods for obtaining the optimal path for a glider vehicle in shallow water and high currents. *Proceedings of the 11th International Symposium on Unmanned Untethered Submersible Technology*. pp. 150-161.
- Garau, B.; Alvarez, A. and Oliver, G. (2005): Path Planning of Autonomous Underwater Vehicles in Current Fields with Complex Spatial Variability: an A\* Approach, *Proceedings of the 2005 IEEE International Conference on Robotics and Automation*, pp. 195-199.
- Holland, W. R. and McWilliams, J. C. (1987): *Computer modelling in physical oceanography from the global circulation to turbulence*. *Physics Today* pp. 51-57.
- Pacanowski, R. C.; K. Dixon, and A. Rosati (1990): Readme file for GFDL-MOM 1.0, *Geophys. Fluid Dyn. Lab., Princeton, N.J.*
- Rio, M-H.; Poulain, P-M.; Pascual, A.; Mauri, E. and Larnicol, G. (2007): A mean dynamic topography of the Mediterranean Sea computed from altimetric data and in-situ measurements. *Journal of Marine Systems*, 65, pp. 484-508



- Robinson, A. R.; Arango, H. G.; Warn-Varnas, A.; Leslie, W. G.; Miller, A. J.; Haley, P. L. and Lozano, C. J. (1996): *Real-time regional forecasting*. Modern approaches to data assimilation in ocean modeling, Amsterdam, NL: Elsevier, pp. 377-410.
- Ruiz, S.; Pascual, A.; Garau, B.; Faugere, Y.; Alvarez, A. and Tintoré, J. (2008): Mesoscale dynamics of the Balearic front integrating glider and satellite data. *Journal of Marine Systems*. In press.
- Schmidt, H. and Bovio, E. (2000): Underwater vehicle networks for acoustic and oceanographic measurements in the littoral ocean. *Proceedings of the 5th IFAC Conference Manoeuvring and Control of Marine Craft (MCMC2000)* pp. 323-326.
- Sugihara, K. and Yuh, J. (1997): GA-based motion planning for underwater robotic vehicle. *Proceedings of the 10th International Symposium on Unmanned Untethered Submersible Technology*, pp. 406-415.
- Vasudevan, C. and Ganesan, K. (1996): *Case-based path planning for autonomous underwater vehicles*. Autonomous Robots. pp. 79-89.
- Warren, C. W. (1990). A technique for autonomous underwater vehicle route planning. *IEEE Journal of Oceanic. Engineering*. vol. 15, pp. 199-204.

